Supporting Information

Identification of Stable Adsorption Sites and Diffusion Paths on Nanocluster Surfaces: An Automated Scanning Algorithm

Tibor Szilvási[†], Benjamin W.J. Chen[†], Manos Mavrikakis*

Department of Chemical Engineering, 1415 Engineering Drive, University of Wisconsin−Madison, Madison, WI 53706, USA

[†] Equal contribution of the authors.

* Corresponding author. Email address: emavrikakis@wisc.edu

Table of Contents

1. Supplementary Figures

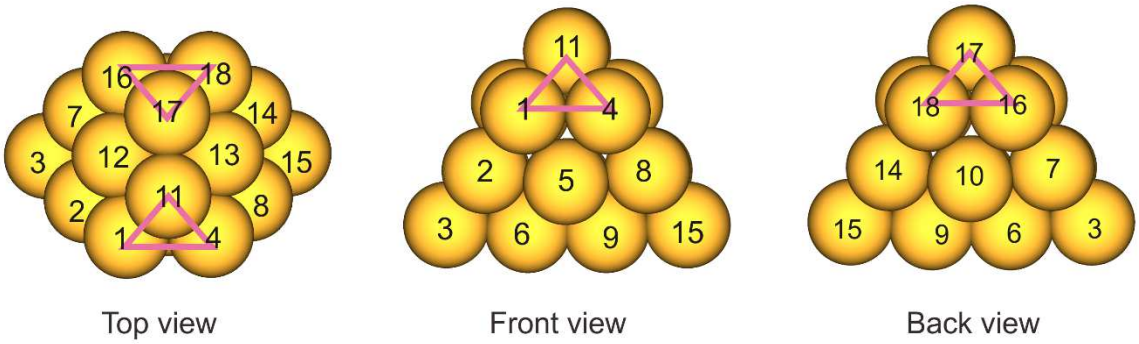

Supplementary Figure 1. Top, front, and back views of Au_{18} with all Au atoms labeled with numbers. The labels are consistent throughout all three views.

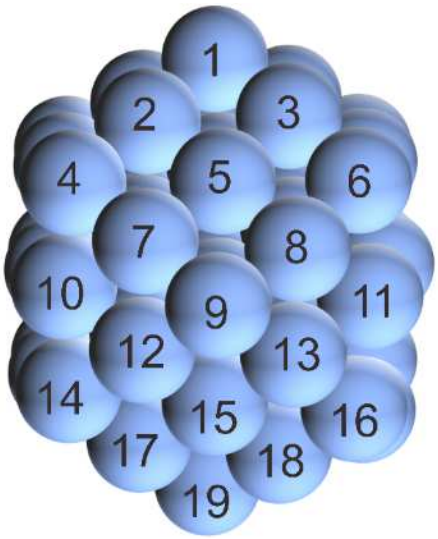

Supplementary Figure 2. Pt_{55} with the Pt atoms labeled.

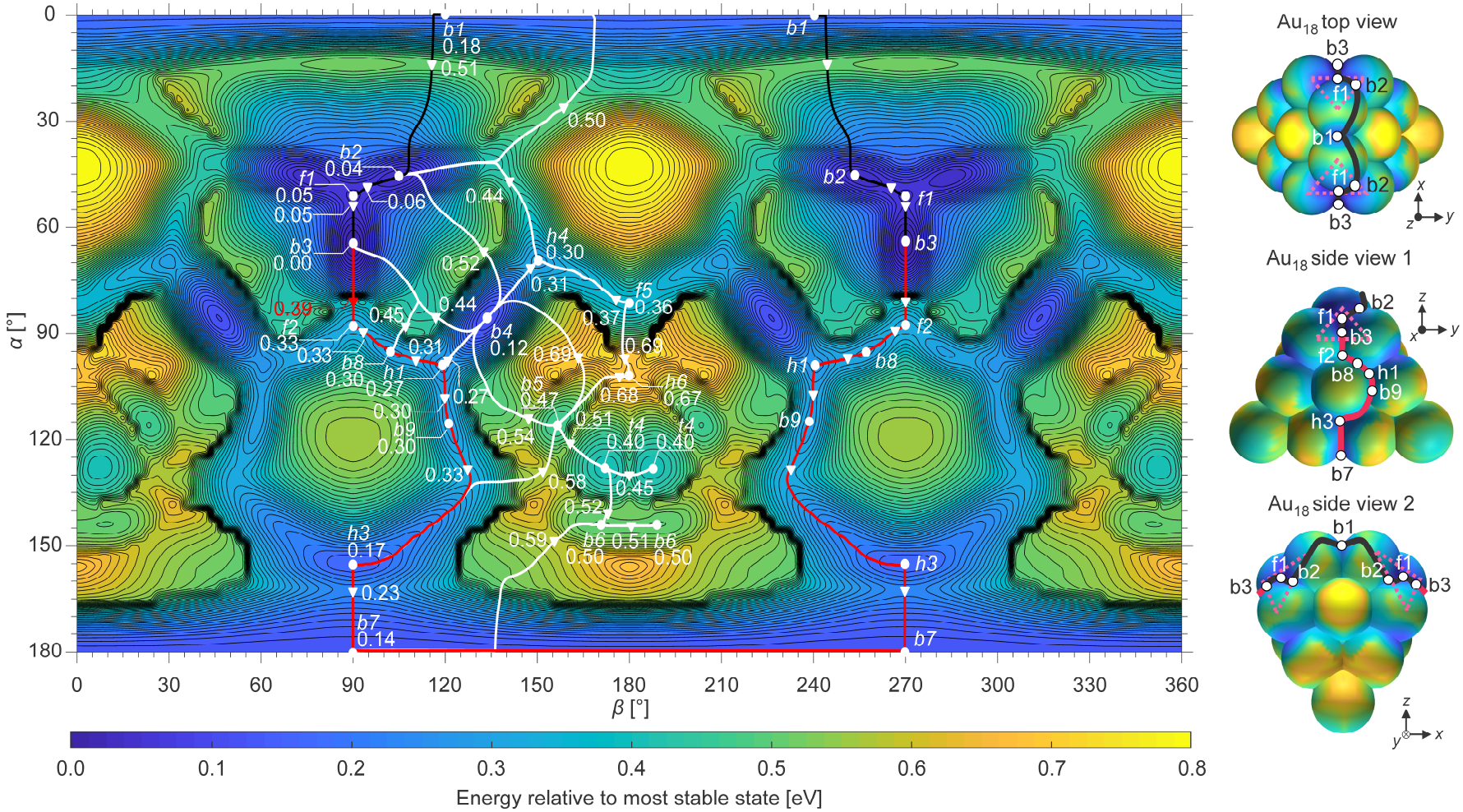

Supplementary Figure 3. Contour-plot and cluster-projected representations of the PES obtained from the Automated Cluster Surface Scanning (ACSS) method for the Au_{18} + H system. White lines are the Minimum Energy Paths connecting transition states (triangles) and minima (circles with site names). Energies are relative to the most stable site. Red lines mark the most energetically favorable diffusion pathway between the two most stable adsorption sites (*b3*); the maximum energy transition state in the most energetically favorable diffusion pathway is also highlighted in red. Black lines mark the spatially shortest diffusion path between the two most stable adsorption sites. Axes for the cluster-projected representations define the frame of reference. Dotted pink triangles mark the two triangular ensembles of Au atoms in Au_{18}, identical to those in Supplementary Figure 1. Definitions of the site types can be found in Supplementary Table 4. A three-dimensional representation of the most energetically favorable diffusion pathway on the Au_{18}cluster is shown in Figure 6 of the main text.

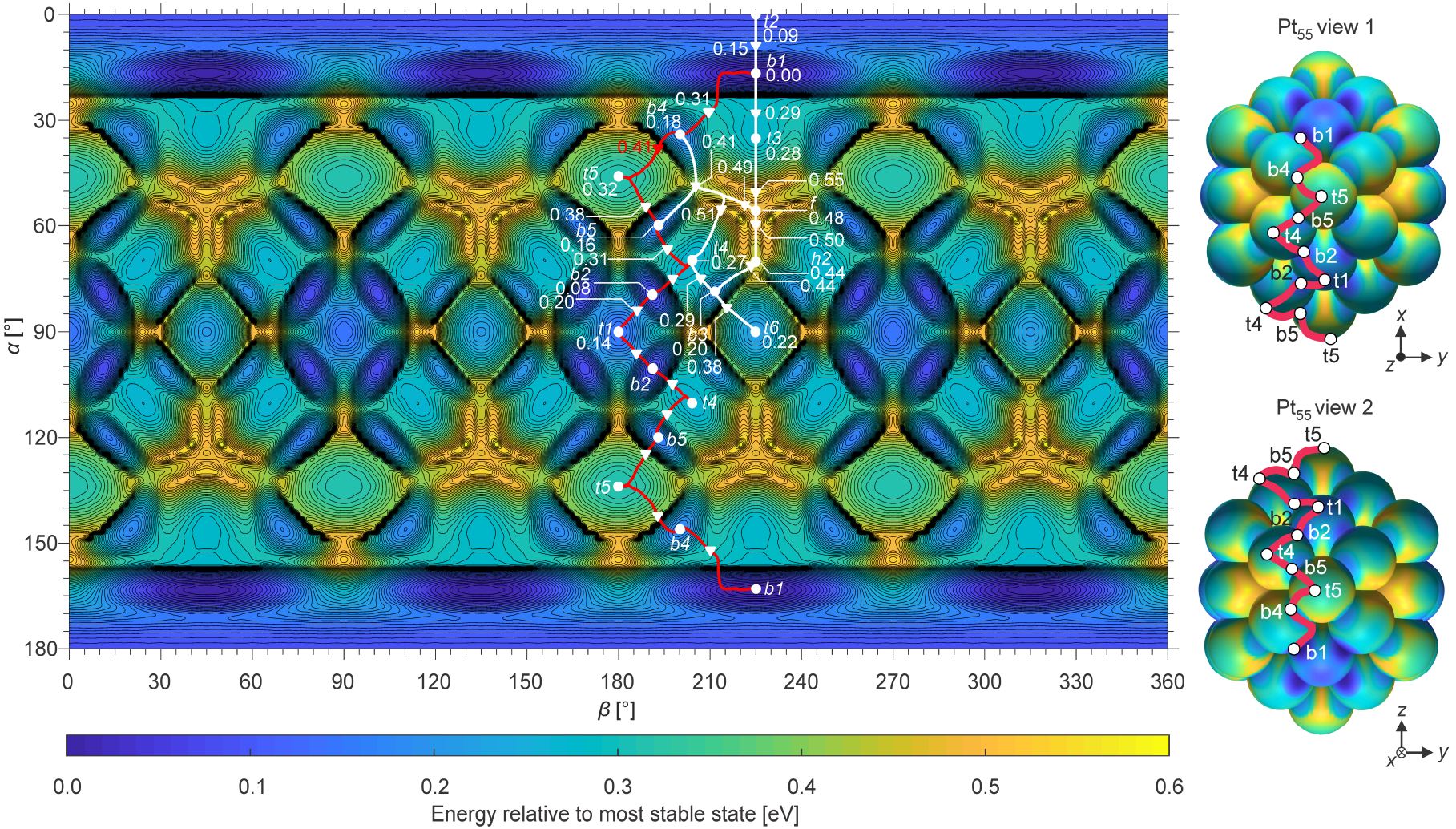

Supplementary Figure 4. Contour-plot and cluster-projected representations of the PES obtained from the Automated Cluster Surface Scanning (ACSS) method for the Pt_{55} + H system. White lines are the Minimum Energy Paths connecting transition states (triangles) and minima (circles with site names). Energies are relative to the most stable site. Red lines mark the most energetically favorable diffusion pathway between the two most stable adsorption sites (*b1*); the maximum energy transition state in the most energetically favorable diffusion pathway is also highlighted in red. Axes for the cluster-projected representations define the frame of reference. Definitions of the site types can be found in Supplementary Table 7. A three-dimensional representation of the most energetically favorable diffusion pathway on the Pt_{55} cluster is shown in Supplementary Figure 5.

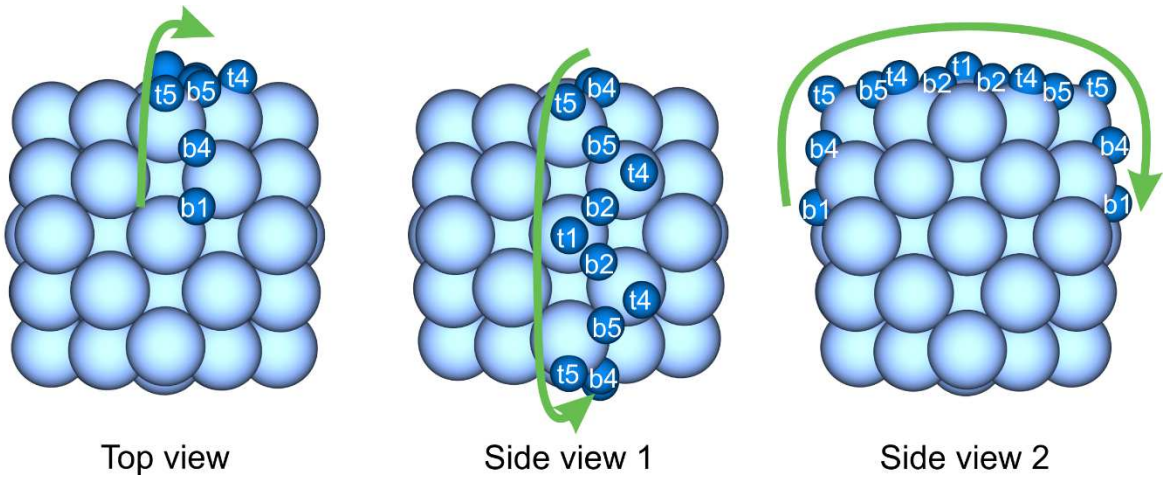

Supplementary Figure 5. Diffusion paths of atomic H on Pt_{55}. Green arrows indicate the most energetically favorable diffusion path between the two most stable *b1* sites, which has an overall barrier of 0.38 eV with respect to the global minimum. Blue spheres represent stable H adsorption sites; light blue spheres represent Pt_{55} atoms. Side view 2 is rotated by 90° with respect to side view 1.

2. Supplementary Discussion

2.1 Convergence of results with respect to the (α, β) mesh

To determine how the number of sampled (α, β) mesh points affects the constructed PESs, we studied how the PESs for the Au_{18} +H system would look like using (α, β) meshes with equidistant 3°, 6°, and 12° intervals in both α, β (Supplementary Figure 6), and how they would look like for the Pt_{55} +H system using (α, β) meshes with 2°, 4°, and 8° intervals in both α, β (Supplementary Figure 8). For each system, the coarser meshes have only 1/4 and 1/16 the points of the finest mesh.

The differences between the PESs obtained with the finest mesh and the coarser meshes are plotted in Supplementary Figure 7 for Au_{18} and in Supplementary Figure 9 for Pt_{55}. These difference plots show how the results evolve with changing the number of sampled points. All PES plots are similar to each other and there are no considerable qualitative differences between them. Importantly, the difference plots confirm that most regions are similarly described for all mesh sizes, with differences smaller than 0.1 eV.

We also calculated the average *interpolation error*, defined as the Root Mean Square Error (RMSE) of energies of all the mesh points that were explicitly calculated in the finest meshes but were derived via interpolation for the coarser meshes. Based on this definition, we calculated an average interpolation error of 0.04 eV for Au_{18} when the mesh with 12° intervals was used (compared with the mesh with 3° intervals), and a similar error of 0.04 eV for Pt_{55} when the mesh with 8° intervals was used (compared with the mesh with 2° intervals). For all other cases, the average interpolation error was even smaller. We thus suggest using coarser meshes when limited by computational resources, as these still provide relatively accurate results.

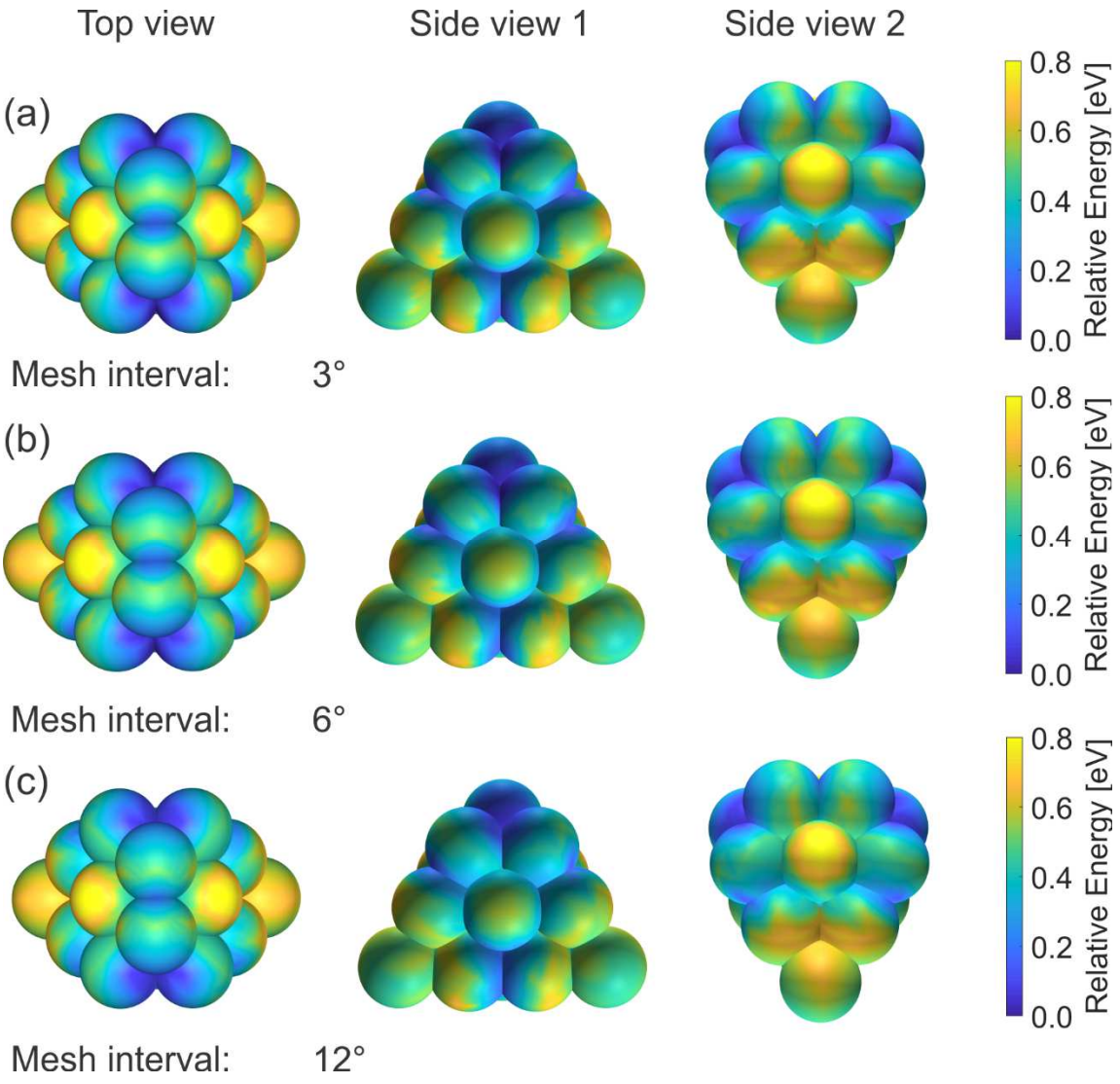

Supplementary Figure 6. *Cluster-projected* representation of the PES obtained from the Automated Cluster Surface Scanning (ACSS) method for the Au_{18} + H system using the (a) 3° equidistant mesh, (b) 6° equidistant mesh, and (c) 12° equidistant mesh.

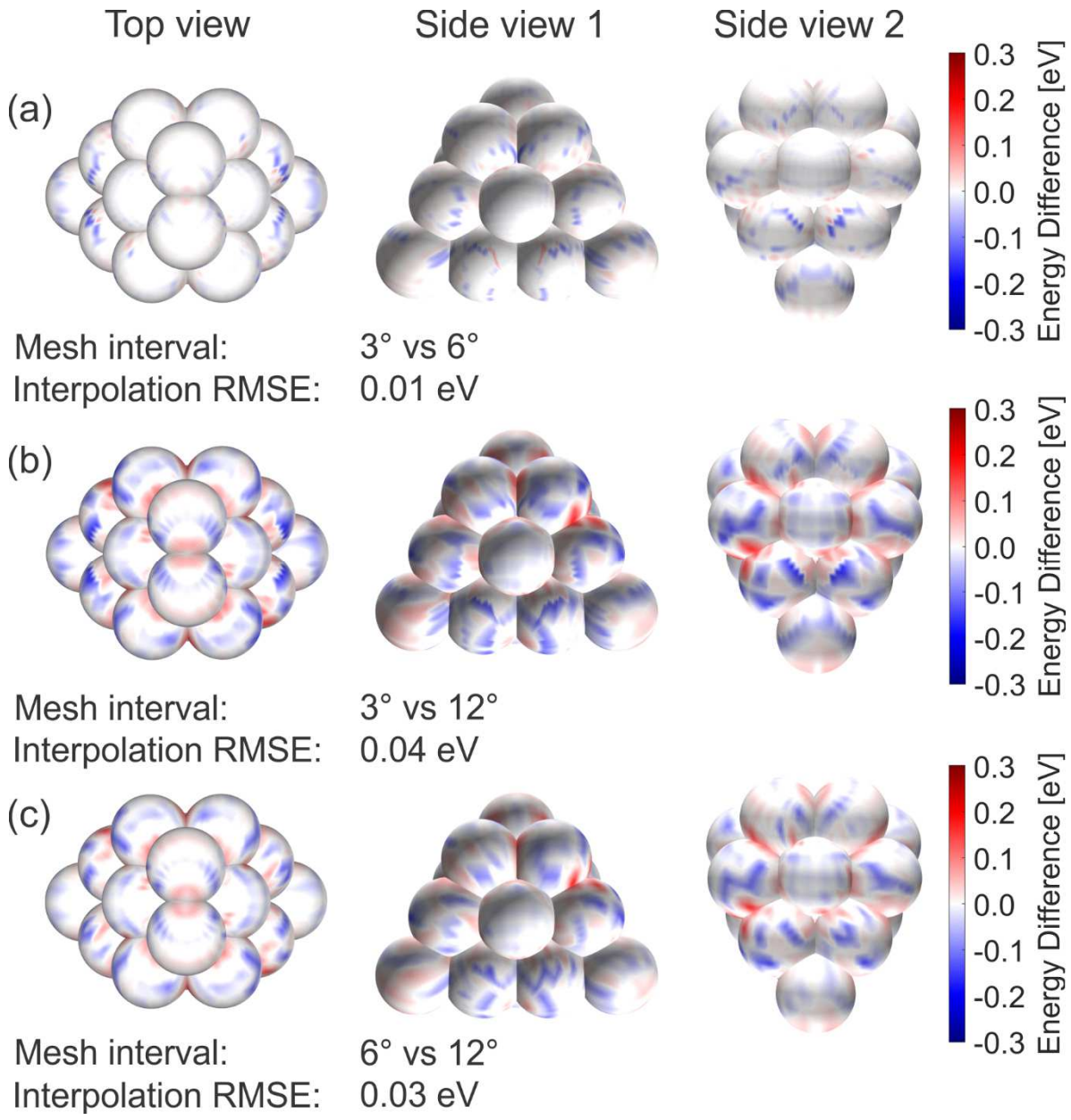

Supplementary Figure 7. *Cluster-projected* representation of the energy differences between PESs obtained from the Automated Cluster Surface Scanning (ACSS) method for the Au_{18} + H system. (a) 3° versus 6° equidistant meshes, (b) 3° versus 12° equidistant meshes, and (c) 6° versus 12° equidistant meshes. The interpolation root mean square error (RMSE) is the RMSE of the energies of all mesh points that were explicitly calculated in the finest meshes but were derived via interpolation for the coarser meshes.

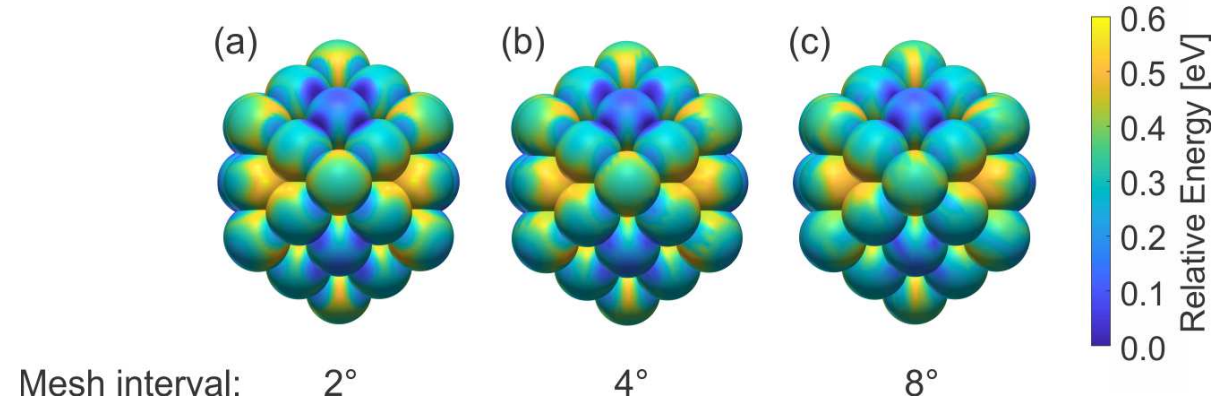

Supplementary Figure 8. *Cluster-projected* representation of the PES obtained from the Automated Cluster Surface Scanning (ACSS) method for the Pt_{55} + H system using the (a) 2° equidistant mesh, (b) 4° equidistant mesh, and (c) 8° equidistant mesh.

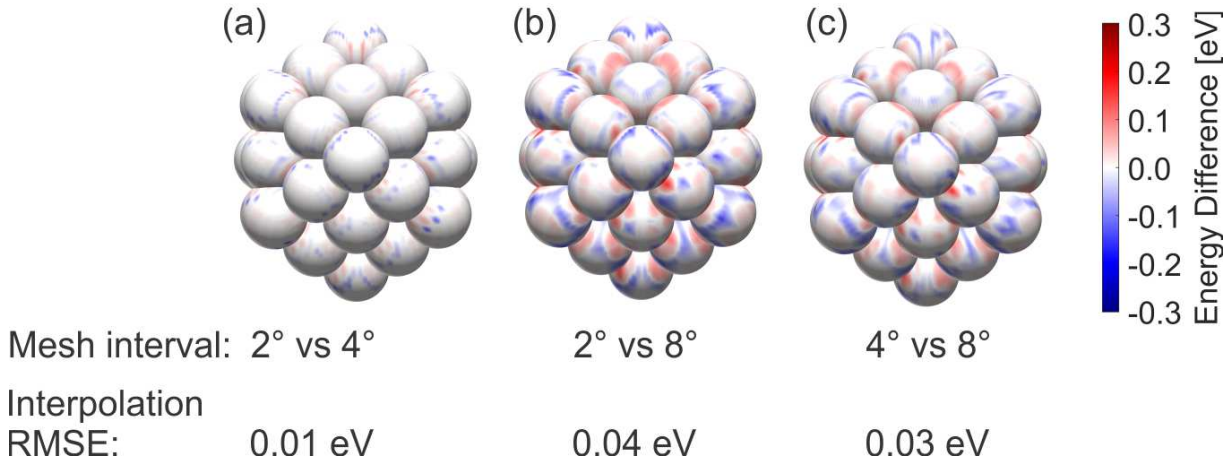

Supplementary Figure 9. *Cluster-projected* representation of the energy differences between the PESs obtained from the Automated Cluster Surface Scanning (ACSS) method for the Pt_{55} + H system. (a) 2° versus 4° equidistant meshes, (b) 2° versus 8° equidistant meshes, and (c) 4° versus 8° equidistant meshes. The interpolation root mean square error (RMSE) is the RMSE of the energies of all mesh points that were explicitly calculated in the finest meshes but were derived via interpolation for the coarser meshes.

2.2 Calculation of Computational Cost

To evaluate the computational cost of MP and ACSS calculations, we monitored the number of geometry optimization steps (Supplementary Table 1) required to complete all MP and ACSS calculations. We chose this metric instead of the number of core hours used as it is easier to track and is independent from computational hardware and software environments.

Supplementary Table 1. Comparison of computational cost of Automated Cluster Surface Scanning (ACSS) calculations versus Manually-Performed calculations with all the atoms in the clusters fully relaxed (MP Relaxed) or with some atoms, the same as those in the ACSS calculations, fixed (MP Fixed). We show the total number of geometric iteration steps required to complete all MP and ACSS calculations and a breakdown in terms of NEB and minima calculations.

	Number of Geometric Iterations					
	Au_{18}			Pt_{55}		
	Total	NEB	Minima	Total	NEB	Minima
MP Relaxed	54909	53424 (97.3%)	1485 (2.7%)	131812	129991 (98.6%)	1821 (1.4%)
MP Fixed	37384	36086 (96.5%)	1298 (3.5%)	85359	83987 (98.4%)	1372 (1.6%)
ACSS	35556	-	-	17479	-	-

For an unbiased estimate of the computational cost, we tracked and archived all nudged-elastic band (NEB) and minima calculations from the very beginning of the project, including non-productive calculations — such as failed, non-converged, or exploratory calculations — as they all contribute to the total computational cost required to carry out the project.

These non-productive calculations, which may account for a significant portion of the total computational cost of MP calculations, arise as we do not have knowledge of which calculations will be productive. For example, when exploring diffusion paths, one must consider all potential pairs of neighboring sites, leading to a vast number of NEB calculations, only a small fraction of which are actual minimum energy paths. Additionally, good initialization of images in NEB calculations is also crucial; inaccurate initial guesses can easily lead to unsuccessful calculations.

On the other hand, the logical simplicity and predetermined nature of ACSS calculations, together with its ability to leverage robust geometry optimization algorithms with good initial guesses, lead to almost all calculations being productive. This is one reason why ACSS calculations are competitive with MP calculations in terms of computational cost.

3. Supplementary Tables

Supplementary Table 2. ACSS versus MP energies for minima of H adsorption on Au_{18}. Dashes indicate sites that are not local minima in MP/ACSS calculations. All energies are in eV. The most stable adsorption site is bolded.

	ACSS Energy	MP Energy	Error
Site	Relative to Global Minimum	Relative to Global Minimum	Relative to Global Minimum
t1	-	-	-
t2	-	-	-
t3	-	-	-
t4	0.40	0.44	0.04
t5	-	-	-
t6	-	-	-
t7	-	-	-
b1	0.18	0.19	0.00
b2	0.04	0.07	0.03
b3	**0.00**	**0.00**	**0.00**
b4	0.12	0.15	0.03
b5	0.47	0.51	0.05
b6	0.50	0.55	0.05
b7	0.14	0.18	0.04
b8	0.30	0.27	-0.03
b9	0.30	0.31	0.01
b10	-	-	-
b11	-	-	-
b12	-	-	-
b13	-	0.30	-
b14	-	-	-
b15	-	-	-
h1	0.27	0.28	0.01
h2	-	-	-
h3	0.17	0.19	0.02
h4	0.30	0.27	-0.03
h5	-	-	-
h6	0.67	0.72	0.05
f1	0.05	0.07	0.02
f2	0.33	0.33	0.00
f3	-	-	-
f4	-	-	-
f5	0.36	0.38	0.01
		Root Mean Square Error	0.03
		Mean Signed Error	0.02

Supplementary Table 3. ACSS versus MP energies for transition states of H diffusion on Au_{18}. Barriers are calculated relative to the more stable initial state of the specific diffusion path. Dashes indicate transition states which are not found. Underscores with numbers, in the name listed in the "Site" column, differentiate between multiple transition states between the same pair of sites. All energies are in eV. Paths belonging to the most energetically favorable diffusion path between the two most stable sites (*b3*), as highlighted in Figure 6 of the main text, are bolded.

	ACSS Energy		MP Energy		Error	
Site	Relative to Global Minimum	Barrier	Relative to Global Minimum	Barrier	Relative to Global Minimum	Barrier
b2-b1_1	0.51	0.47	0.52	0.45	0.00	-0.03
b2-b1_2	0.50	0.46	0.45	0.39	-0.04	-0.07
b2-b4	0.52	0.48	0.55	0.48	0.03	0.00
b2-f1	0.06	0.02	0.07	0.01	0.02	-0.01
b2-h4	0.44	0.40	0.41	0.34	-0.03	-0.06
b3-b4	0.44	0.44	0.47	0.47	0.03	0.03
b3-f1	0.05	0.05	0.07	0.07	0.02	0.02
b3-f2	**0.39**	**0.39**	**0.41**	**0.41**	**0.02**	**0.01**
b3-b8	0.45	0.45	0.47	0.47	0.02	0.02
b4-b5_1	0.54	0.42	0.58	0.43	0.03	0.01
b4-b5_2	0.69	0.57	0.75	0.61	0.06	0.03
b4-h1	0.27	0.16	0.28	0.14	0.01	-0.02
b4-h4	0.31	0.19	0.30	0.15	-0.01	-0.04
b5-h3	0.58	0.41	0.62	0.43	0.04	0.02
b5-h6	0.68	0.22	0.72	0.21	0.04	-0.01
b5-t4	0.51	0.11	0.72	0.27	0.20	0.16
b6-b6	0.51	0.01	0.56	0.01	0.05	0.00
b6-b7	0.59	0.45	0.62	0.44	0.03	-0.01
b6-t4	0.52	0.12	0.68	0.24	0.16	0.12
b7-h3	**0.23**	**0.09**	**0.26**	**0.08**	**0.03**	**-0.02**
b8-f2	**0.33**	**0.03**	**0.33**	**0.06**	**0.00**	**0.03**
b8-h1	**0.31**	**0.04**	**0.30**	**0.03**	**-0.01**	**-0.01**
b9-h1	**0.30**	**0.03**	**0.31**	**0.02**	**0.00**	**0.00**
b9-h3	**0.33**	**0.16**	**0.35**	**0.16**	**0.02**	**0.01**
b13-f5*	0.37	0.10	0.38	0.07	0.01	0.03
b13-h4*	-	-	0.30	0.03	-	-
f5-h6	0.69	0.33	0.72	0.35	0.03	0.02
h3-t4	0.58	0.41	0.68	0.48	0.10	0.08
t4-t4	0.45	0.05	0.46	0.01	0.00	-0.04
			Root Mean Square Error		0.06	0.05
			Mean Signed Error		0.03	0.01

*ACSS missed the shallow minimum b13, thus although in MP calculations there are paths f5-b13 and b13, in ACSS there is only the f5-h4 path. The transition state that ACSS found for this path corresponds to the transition state of the b13-f5 path in MP calculations.

Supplementary Table 4. Definition of sites for H adsorption on Au_{18}. The column "Atoms" denotes the indices of the Au atoms coordinated to the sites, as represented in Supplementary Figure 1. Dashes indicate sites that are not local minima in ACSS calculations. M/A indicates whether a site is a local minimum in MP (M) or ACSS (A) calculations, respectively. "t", "b", "f", and "h" site types represent top, bridge, fcc-like hollow, and hcp-like hollow site types respectively. The most stable adsorption site is bolded.

Site	Atoms	Alpha	Beta	Minima in MP/ACSS
t1	1	-	-	-
t2	11	-	-	-
t3	2	-	-	-
t4	3	128	172	M/A
t5	6	-	-	-
t6	5	-	-	-
t7	12	-	-	-
b1	11,17	0	120	M/A
b2	1,11	46	105	M/A
b3	**1,4**	**65**	**90**	**M/A**
b4	1,2	86	134	M/A
b5	2,3	116	157	M/A
b6	3,6	144	171	M/A
b7	6,9	180	90	M/A
b8	1,5	95	102	M/A
b9	2,5	115	121	M/A
b10	5,6	-	-	-
b11	2,6	-	-	-
b12	2,7	-	-	-
b13	2,12	-	-	M
b14	1,12	-	-	-
b15	11,12	-	-	-
h1	4,5,8	99	119	M/A
h2	8,9,15	-	-	-
h3	5,6,9	155	90	M/A
h4	1,2,12	69	150	M/A
h5	11,12,17	-	-	-
h6	2,3,7	102	180	M/A
f1	1,4,11	51	90	M/A
f2	1,4,5	88	90	M/A
f3	5,8,9	-	-	-
f4	1,11,12	-	-	-
f5	2,7,12	81	180	M/A

Supplementary Table 5. ACSS versus MP energies for H adsorption minima on Pt_{55}. Dashes indicate sites that are not local minima in MP/ACSS calculations. All energies are in eV. The most stable adsorption site is bolded.

	ACSS Energy	MP Energy	Error
Site	Relative to Global Minimum	Relative to Global Minimum	Relative to Global Minimum
t1	0.14	0.14	0.00
t2	0.09	0.09	0.00
t3	0.28	0.25	-0.03
t4	0.27	0.25	-0.02
t5	0.32	0.26	-0.05
t6	0.22	0.20	-0.01
b1	**0.00**	**0.00**	**0.00**
b2	0.08	0.07	0.00
b3	0.20	0.18	-0.03
b4	0.18	0.17	-0.01
b5	0.16	0.16	0.00
b6	-	-	-
b7	-	-	-
h1	-	-	-
h2	0.44	0.41	-0.03
h3	-	-	-
h4	-	-	-
h5	-	-	-
f	0.48	0.47	-0.01
		Root Mean Square Error	0.02
		Mean Signed Error	-0.01

Supplementary Table 6. ACSS versus MP energies for transition states of H diffusion on Pt_{55}. Barriers are calculated relative to the more stable initial state of the reaction path. All energies are in eV. Paths belonging to the most energetically favorable diffusion path between the two most stable sites (*b1*), as highlighted in Supplementary Figure 5, are bolded.

	ACSS Energy		MP energy		Error	
Site	Relative to Global Minimum	Barrier	Relative to Global Minimum	Barrier	Relative to Global Minimum	Barrier
b1-b4	**0.31**	**0.31**	**0.29**	**0.29**	**-0.02**	**-0.02**
b1-t2	0.15	0.15	0.15	0.15	0.00	0.00
b1-t3	0.29	0.29	0.29	0.29	0.00	0.00
b2-t1	**0.20**	**0.13**	**0.20**	**0.12**	**-0.01**	**0.00**
b2-t4	**0.29**	**0.21**	**0.29**	**0.21**	**0.00**	**0.00**
b3-h2	0.44	0.24	0.41	0.23	-0.03	-0.01
b3-t4	0.29	0.08	0.28	0.10	0.00	0.01
b3-t6	0.38	0.18	0.38	0.20	0.00	0.02
b4-b5	0.41	0.23	0.40	0.24	-0.01	0.01
b4-t5	**0.41**	**0.23**	**0.38**	**0.20**	**-0.03**	**-0.02**
b5-t4	**0.31**	**0.15**	**0.28**	**0.12**	**-0.03**	**-0.03**
b5-t4_1	0.51	0.35	0.52	0.36	0.01	0.01
b5-t5	**0.38**	**0.22**	**0.38**	**0.21**	**-0.01**	**-0.01**
b5-f	0.49	0.33	0.50	0.34	0.01	0.01
h2-f	0.50	0.06	0.47	0.06	-0.03	0.00
t3-f	0.55	0.27	0.50	0.25	-0.04	-0.02
			Root Mean Square Error		0.02	0.01
			Mean Signed Error		-0.01	0.00

Supplementary Table 7. Definition of sites for H adsorption on Pt_{55}. The column "Atoms" denotes the indices of the Pt atoms coordinated to the sites, as represented in Supplementary Figure 2. Dashes indicate sites that are not local minima in ACSS calculations. M/A indicates whether a site is a local minimum in MP (M) or ACSS (A) calculations, respectively. "t", "b", "f", and "h" site types represent top, bridge, fcc-like hollow, and hcp-like hollow site types respectively. The most stable adsorption site is bolded.

Site	Atoms	Alpha	Beta	Minima in MP/ACSS
t1	15	90	0	M/A
t2	5	0	44	M/A
t3	7	34	44	M/A
t4	12	68	24	M/A
t5	9	46	0	M/A
t6	14	90	44	M/A
b1	**5, 7**	**16**	**44**	**M/A**
b2	12, 15	80	10	M/A
b3	12, 14	80	30	M/A
b4	7, 9	34	20	M/A
b5	9, 12	60	12	M/A
b6	7, 12	-	-	-
b7	10, 12	-	-	-
h1	7,9,12	-	-	-
h2	10,12,14	70	44	M/A
h3	5,7,8,9	-	-	-
h4	9,12,13,15	-	-	-
h5	12,14,15,17	-	-	-
f	7,10,12	56	44	M/A

Supplementary Table 8. Optimized coordinates of the naked Au_{18} cluster. Both ACSS and MP calculations use the same optimized cluster coordinates.

Atom Number	Coordinates / Å		
	x	*y*	*z*
1	7.920367	7.574070	10.097662
2	10.518748	8.195125	9.980337
3	13.198978	8.485768	9.840013
4	6.423121	7.382640	7.705021
5	9.010471	8.592478	7.660642
6	11.845896	8.413202	7.461172
7	12.364469	6.061538	8.995084
8	7.625149	7.824543	5.357847
9	10.448934	8.233505	5.228805
10	11.410262	5.816618	6.376953
11	6.817100	5.138101	9.310854
12	9.610482	5.472503	9.637881
13	7.722349	5.229385	6.627391
14	9.466308	5.688958	4.371244
15	8.910322	7.938616	2.985830
16	11.250347	3.725945	8.317885
17	8.519403	3.167123	8.402267
18	9.753834	3.533033	5.927166

Supplementary Table 9. Optimized coordinates of the naked Pt_{55} cluster. Both ACSS and MP calculations use the same optimized cluster coordinates.

Atom Number	Coordinates / Å		
	x	*y*	*z*
1	3.868580	6.603514	5.813500
2	3.911097	6.591067	9.647393
3	3.866741	10.434106	5.828189
4	3.906245	10.422390	9.655902
5	7.668783	6.562475	5.729984
6	7.708842	6.549551	9.647926
7	7.664799	10.481157	5.743533
8	7.705218	10.471821	9.661136
9	11.468675	6.608043	5.738610
10	11.507561	6.597200	9.560583
11	11.465101	10.444028	5.747983
12	11.502544	10.429951	9.579190
13	4.052162	4.681822	7.721631
14	4.008298	8.526362	3.900853
15	3.710399	8.511694	7.738949
16	4.095542	8.503093	11.570094
17	4.050233	12.349370	7.745474
18	7.648014	4.634916	3.783195
19	7.687342	4.376684	7.681900
20	7.729158	4.604026	11.580504
21	7.647626	8.526353	3.559148
22	7.687272	8.516199	7.694630
23	7.732773	8.504394	11.832476
24	7.643790	12.419897	3.808439
25	7.684843	12.656910	7.710725
26	7.723698	12.404969	11.608685
27	11.321629	4.678099	7.644292
28	11.287439	8.530466	3.828518
29	11.665282	8.522749	7.654553
30	11.359022	8.506395	11.490854
31	11.318532	12.355617	7.672057
32	5.816469	6.568576	3.734976
33	5.836665	6.572213	7.708302
34	5.903195	6.541407	11.682980
35	5.815109	10.484468	3.747195
36	5.834499	10.458034	7.721344
37	5.898383	10.465862	11.692329
38	9.482040	6.566243	3.702019

39	9.539434	6.573624	7.669267
40	9.560008	6.540742	11.639786
41	9.476237	10.489549	3.711158
42	9.535276	10.462248	7.683763
43	9.555712	10.469954	11.655341
44	5.838066	4.548223	5.739748
45	5.879942	4.535184	9.663973
46	5.814817	8.520280	5.771963
47	5.856730	8.508751	9.657301
48	5.835094	12.493486	5.765420
49	5.874859	12.485275	9.689451
50	9.496370	4.547168	5.702000
51	9.538905	4.536786	9.624607
52	9.520038	8.524217	5.735560
53	9.556522	8.511991	9.617084
54	9.492184	12.496465	5.727877
55	9.533169	12.487661	9.653154